ARTICLE
Journal of Cellular Biochemistry 105:712–723 (2008)

Journal of Cellular Biochemistry

PK 11195 Differentially Affects Cell Survival in Human Wild-Type and 18 kDa Translocator Protein-Silenced ADF Astrocytoma Cells

Beatrice Chelli,[1] Alessandra Salvetti,[2] Eleonora Da Pozzo,[1] Mariarosa Rechichi,[2] Francesca Spinetti,[1] Leonardo Rossi,[2] Barbara Costa,[2] Annalisa Lena,[2] Giuseppe Rainaldi,[3] Fabrizio Scatena,[4] Renato Vanacore,[4] Vittorio Gremigni,[2] and Claudia Martini[1]*

[1]*Department of Psychiatry, Pharmacology, Neurobiology and Biotechnology, University of Pisa, Pisa, Italy*
[2]*Department of Human Morphology and Applied Biology, University of Pisa, Pisa, Italy*
[3]*Laboratory of Gene and Molecular Therapy, Institute of Clinical Physiology, CNR, Pisa, Italy*
[4]*U.O. Immunohaematology 2, Cisanello Hospital, Pisa, Italy*

ABSTRACT

Gliomas are the most common brain tumours with a poor prognosis due to their aggressiveness and propensity for recurrence. The 18 kDa translocator protein (TSPO) has been demonstrated to be greatly expressed in glioma cells and its over-expression has been correlated with glioma malignance grades. Due to both its high density in tumours and the pro-apoptotic activity of its ligands, TSPO has been suggested as a promising target in gliomas. With the aim to evidence if the TSPO expression level alters glioma cell susceptibility to undergo to cell death, we analysed the effects of the specific TSPO ligand, PK 11195, in human astrocytoma wild-type and TSPO-silenced cell lines. As first step, TSPO was characterised in human astrocytoma cell line (ADF). Our data demonstrated the presence of a single class of TSPO binding sites highly expressed in mitochondria. PK 11195 cell treatment activated an autophagic pathway followed by apoptosis mediated by the modulation of the mitochondrial permeability transition. In TSPO-silenced cells, produced by siRNA technique, a reduced cell proliferation rate and a decreased cell susceptibility to the PK 11195-induced anti-proliferative effect and mitochondrial potential dissipation were demonstrated respect to control cells. In conclusion, for the first time, PK 11195 was demonstrated to differentially affect glioma cell survival in relation to TSPO expression levels. These results encourage the development of specific-cell strategies for the treatment of gliomas, in which TSPO is highly expressed respect to normal cells. J. Cell. Biochem. 105: 712–723, 2008.

KEY WORDS: TSPO; GLIOMA; AUTOPHAGY; APOPTOSIS; MITOCHONDRIAL MEMBRANE POTENTIAL; RNA INTERFERENCE

Malignant gliomas are the most devastating neoplasms that account for almost half of all primary brain tumours. In the central nervous system (CNS) their aggressive infiltration typically produces progressive and profound disability, leading to death in nearly all cases. Despite modern advances in surgery, radio- and chemotherapies, the treatment of these tumours has so far a limited success [Stern and Raizer, 2006]. Since the deregulation of apoptotic cell death process is reported to be involved both in the tumourigenicity and in the development of chemotherapy resistance, the induction and/or the enhancement of apoptosis have been suggested to probably constitute a promising approach achieving a major anti-tumoural efficacy. The 18 kDa translocator protein (TSPO), the current name for the peripheral-type benzodiazepine receptor [Papadopoulos et al., 2006a], has been suggested as a potential anti-cancer drug target [Galiegue et al., 2003; Decaudin, 2004]. The rationale behind this potential application is based on two main features. Firstly, it has been postulated TSPO represents a component of the mitochondrial permeability transition pore (PTP) [Zoratti and Szabo, 1995], that plays a key role in the control of cell death pathways [Casellas et al., 2002]. Indeed, several TSPO ligands, modulating the opening of the PTP, show anti-proliferative and pro-apoptotic activities in various different tumoural cells [Galiegue et al., 2003; Decaudin, 2004; Papadopoulos et al., 2006b]. In this line, our previous data evidenced that classical TSPO ligands, such as

B. Chelli and A. Salvetti contributed equally to this work.

Grant sponsor: MIUR, Italy (2004); Grant number: prot. 2004034317.

*Correspondence to: Dr. Claudia Martini, Department of Psychiatry, Pharmacology, Neurobiology and Biotechnology, University of Pisa, Via Bonanno 6, Pisa 56126, Italy. E-mail: cmartini@farm.unipi.it

Received 20 December 2007; Accepted 23 June 2008 • DOI 10.1002/jcb.21865 • 2008 Wiley-Liss, Inc.
Published online 30 July 2008 in Wiley InterScience (www.interscience.wiley.com).

the isochinolincarboxamide derivative PK 11195 and the benzodiazepine Ro5-4864 [Chelli et al., 2004], as well as the newly synthesised 2-phenylindolilglyoxylamide derivative PIGA [Chelli et al., 2005] induce apoptosis via PTP in rat C6 glioma cells and in human Jurkat leukaemia cells [Costa et al., 2006]. Secondly, TSPO expression has been found to be increased in several tumours and cancer cell lines relative to untransformed cells. A positive correlation between TSPO expression levels and tumourigenicity of cancer cells, including gliomas, has been also documented leading to the hypothesis that the presence of TSPO may be a determinant factor for the aggressive phenotypes [Hardwick et al., 1999; Brown et al., 2000; Veenman and Gavish, 2006; Vlodavsky and Soustiel, 2007]. However, direct evidences on the relationship between the TSPO density and the anti-proliferative activity of TSPO ligands in tumoural cells are limited.

Therefore, we assessed the ability of the selective and high affinity TSPO ligand PK 11195 to induce cell death in a human astrocytoma cell line (ADF), firstly evaluating [^{3}H]PK 11195 binding parameters and the TSPO subcellular distribution. Furthermore, the relationship between the TSPO expression levels and ADF cell susceptibility to cell death induction was investigated. With this goal, the cell proliferation rate and TSPO ligand effects on cell viability and mitochondrial potential were evaluated in ADF cells engineered to express reduced TSPO levels by short interfering RNA (siRNA) technique.

MATERIALS AND METHODS

MATERIALS

Cell culture media and growth supplements were obtained from Cambrex Bio Science Walkersville, Inc. (Walkersville, MD). One percent non-essential amino acids were from GIBCO (Milan, Italy). Anti-TSPO rabbit polyclonal primary antibody was purchased from Trevigen (Gaithersburg, MD). Monoclonal anti-cytochrome *c*, rhodamine-conjugate anti-rabbit secondary antibody were purchased from Santa Cruz Biotechnology (Santa Cruz, CA). Anti-HSP70 rabbit polyclonal antibody was from Stressgen (San Diego, CA). FITC-conjugate anti-mouse secondary antibody was purchased from Molecular Probes (Leiden, NL). Horseradish peroxidase-conjugated anti-mouse and anti-rabbit secondary antibodies, non-fat dry milk and Protein Assay were from Bio-Rad (Hercules, CA). Cell Death detection ELISA^{PLUS} was purchased from Roche Applied (Monza, Italy). Mitochondria/cytosol fractionation kit was from BioVision (Vinci-Biochem, Italy). Monoclonal anti-HMGB1 antibody was purchased from BD Pharmingen (Franklin Lakes, NJ). Ampli-Scribe T7 high yield transcription kit was from Epicenter Technologies (Madison, WI). SuperSignal West Dura Extended Duration Substrate and Micro BCA protein assay kit were purchased from Pierce Biotechnology, Inc. (Rockford, IL). Scrambled Negative Control Stealth RNA, Lipofectamine 2000 and BLOCK-iT Fluorescent oligo were purchased from Invitrogen (Burlinghton, ON). [^{3}H]PK 11195 (specific activity, 73.6 Ci/mmol) was purchased from PerkinElmer (Waltham, MA); PK 11195 (1-(2-chlorophenyl-*N*-methyl-1-methylpropyl)-3-isoquinolinecarboxamide), Ro5-4864 (7-chloro-5-(4-chlorophenyl)-1,3-dihydro-1-methyl-2H-1,4-benzodiazepin-2-one) diazepam, clonazepam, CCCP (carbonylcyanide-*m*-chlorophenylhydrazone), Lonidamine, protease inhibitors, Triton X-100 and Trypan blue were from Sigma/RBI (Natick, MA). Cell Titer 96 Aqueous One Solution Cell Proliferation assay and JC-1 (5,5′,6,6′-tetrachloro-1,′,3,3′-tetraethylbenzimidazolcarbocianine iodide) were obtained from Promega (Milan, Italy). All other reagents were from standard commercial sources.

ADF CELL CULTURE CONDITIONS

Human ADF astrocytoma cell line [Malorni et al., 1994] was maintained in standard culture conditions (37°C, 95% humidity, 5% CO_2) in RPMI 1640 medium supplemented with 10% fetal bovine serum (FBS), 2 mM L-glutamine, 100 U/ml penicillin, 100 μg/ml streptomycin and 1% non-essential amino acids (complete medium), as previously described [Ceruti et al., 2000].

TSPO CHARACTERISATION IN WILDTYPE ADF CELLS

[^{3}H]PK 11195 binding assays. For crude membrane preparation, confluent ADF cells derived from a 175 cm^2 cell flask were harvested using phosphate buffer saline (PBS), pH 7.4, supplemented with EDTA 0.04%. After cell collection by centrifugation (200*g* for 5 min), the pellet was suspended in ~10 ml of ice-cold buffer Tris–HCl 5 mM, pH 7.4 containing protease inhibitors (160 μg/ml benzamidine, 200 μg/ml bacitracin and 20 μg/ml trypsin inhibitor) and homogenised with an Ultraturrax. Then, homogenate was centrifuged at 48,000*g* for 15 min at 4°C and the supernatant was discarded. The obtained pellet was suspended in ~10 ml of Tris–HCl 50 mM, pH 7.4 (assay buffer) containing the same amounts of protease inhibitors as above described, and the homogenate was pelleted by centrifugation (48,000*g*, 15 min, 4°C). The pellet was washed once with assay buffer and an additional centrifugation step followed (48,000*g*, 15 min, 4°C). The resulting cell membrane pellet was suspended at the final concentration of 1 mg of proteins/ml in assay buffer and used for binding assays. Protein content of 20 μl membrane suspension was measured by the Bradford method [1976] using the Bio-Rad Protein Assay reagent, according to the manufacturer's protocol, with bovine serum albumin (BSA) as standard.

To determine the presence of specific [^{3}H]PK 11195 binding to ADF cell membrane suspensions, equilibrium radioligand binding assays were performed essentially as previously described [Costa et al., 2006]. Briefly, different aliquots of ADF cell membranes (10–100 μg of proteins) were incubated with [^{3}H]PK 11195 (1.5 nM) in the presence (non-specific binding) or in the absence (total binding) of unlabelled PK 11195 (1 μM), in the final volume of 500 μl of assay buffer for 90 min at 0°C. For saturation experiments, aliquots of ADF cell membranes (20 μg of proteins) were incubated in duplicates with eight increasing [^{3}H]PK 11195 concentrations (0.5–30 nM) in the same above described conditions.

In each assay, the final ethanol concentration in the incubation buffer was less than 1% and did not interfere with specific [^{3}H]PK 11195 binding.

TSPO subcellular localisation analyses. Immunocytochemistry experiments were performed essentially as previously described [Costa et al., 2006]. In particular, ADF cells were incubated for 1 h at room temperature with 1:200 anti-TSPO antibody and 1:50

anti-cytochrome *c* antibody. Control cells were incubated in blocking solution with no primary antibody. After washing, the cells were incubated for 1 h at room temperature with 1:200 FITC-conjugate anti-mouse secondary antibody and 1:200 rhodamine-conjugate anti-rabbit secondary antibody in blocking solution. The cells were analysed using an Axioplan (Carl Zeiss, Inc., Thornwood, NJ) epifluorescence microscope.

ADF CELL LINES ENGINEERED TO REDUCE TSPO EXPRESSION

Transfection and RNA interference experiments. Among a series of siRNAs, the most active ones against human TSPO gene (Accession number BC001110), designed according to the guidelines published by Elbashir et al. [2002], were identified using the energy profiling guidelines [Poliseno et al., 2004]. siRNAs were synthesised using the Ampli-Scribe T7 high yield transcription kit according to manufacturer's instructions. The following sequences were used as templates: 5′-AGACCACACTCAACTACTGCTCTCTTGAAGCAG-TAGTTGAGTGTGGTCTATAGTGAGTCGTATTACC-3′, referred to as TSPO-1 siRNA and 5′-AAGTGTCCTGTGCTTTCTGCATCTC-TTGAATGCAGAAAGCACAGGACACTATAGTGAGTCGTATTACC-3′ referred to as TSPO-2 siRNA. ADF cells were transfected at 30% confluence with siRNAs using Lipofectamine 2000 according to the manufacturer's recommendations. After 6 h, medium supplemented with 10% FBS was added and the cells were maintained in culture for further 72 h in the same conditions above described for wt (wild-type) ADF cells, and then used for functional experiments. To optimise transfection conditions BLOCK-iT Fluorescent oligo was used. As negative controls Scramble (Scrambled Negative Control Stealth transfected cells) and Mock cells (cells transfected only with Lipofectamine) were used.

ANALYSES OF TSPO EXPRESSION LEVELS

Flow cytometry assays. To verify the ability of siRNAs to down-regulate TSPO expression in ADF cells, intracellular flow cytometry analysis of the protein levels was initially performed according to Poliseno et al. [2005]. Briefly, 72 h after transfection, wt and transfected ADF cells were trypsinised and fixed with 4% paraformaldehyde in PBS for 20 min at room temperature. Each sample was then divided in two parts. One part (3×10^5 cells) was incubated with a 1:20 dilution of anti-TSPO antibody in blocking buffer (0.00125% Nonidet P-40, 0.5% BSA in PBS) for 1 h at room temperature, then the cells were washed in PBS and successively incubated for 30 min with a 1:50 dilution of a FITC-conjugated anti-rabbit secondary antibody in blocking buffer. The remaining cells were incubated only with the secondary antibody (1:50) and used to measure the fluorescence background. Following incubation times, each sample was analysed with a FASCalibur flow cytometer (Becton Dickinson, USA) using CELL Quest analysis software. The values of TSPO mean fluorescence intensity, diminished of that of the secondary antibody, was determined to quantify the TSPO expression level.

[^{3}H]PK 11195 binding assays. After 72 or 120 h from ADF cell transfection, crude membranes were prepared from TSPO siRNAs or Scramble transfected cells as well as from wt and Mock cells as above described. Then, for each cell line [^{3}H]PK 11195 specific binding was determined by radioligand binding assays, incubating aliquots of each membrane preparation (20 μg of proteins) with [^{3}H]PK 11195 (1 nM) for 90 min at 0°C in 500 μl of assay buffer. Non-specific binding was determined in the presence of unlabelled 1 μM PK 11195.

TSPO FUNCTIONAL STUDIES

PK 11195 cell treatments. For functional experiments, wt or transfected ADF cells, grown on flasks or Petri dishes, were detached by mild trypsinisation and counted using an Axioplan (Carl Zeiss, Inc.,) epifluorescence microscope with the aid of a haemocytometer (Neubauer-counting chamber) and Trypan Blue dye (at a final concentration of 0.1%) to concomitantly determine the percentage of dead cells. Then, cells were seeded in 96-well plates at a density of $\sim 3.5 \times 10^3$/well for proliferation assays or in 24-well plates at a density of $\sim 20 \times 10^3$/well for apoptosis measurements.

In TSPO ligand experiments culture medium was replaced by complete medium supplemented with different PK 11195 concentrations or by complete medium added with ethanol (control cells), and the cells were incubated for various periods of time. Details of the applied concentrations and incubation times are specifically given in the appropriate result section. In each assay, the vehicle (ethanol) in which PK 11195 was dissolved, never exceeded 1% of final assay volume and we verified that this amount did not affect cell survival.

Proliferation analyses by MTS conversion assay. The same number (3.5×10^3) of wt or transfected ADF cells were seeded in 96-well plates and allowed to proliferate for 72 h. At repeated times, the number of viable cells in each ADF cell line was measured by using the quantitative colorimetric MTS conversion assay as previously described [Chelli et al., 2004]. In parallel, cell death was determined by Trypan Blue assay as described above. All measurements were performed in duplicate and the experiments were repeated, at least, three times.

ADF CELL VIABILITY ANALYSES

MTS conversion assay. To assess the effects of TSPO ligand on viability, ADF cells were incubated with different concentrations of PK 11195 for various periods of time. Specifically, wt ADF cells were exposed to increasing PK 11195 concentrations (ranging from 1 nM to 100 μM) for 2, 6, 12, 24 or 48 h. In the experiments carried out on TSPO silenced and control cells, wt, Mock, Scramble and TSPO-2 transfected cells were incubated in the absence or in the presence of increasing PK 11195 concentrations (ranging from 10 to 100 μM) for different intervals of time (6, 12, 24 or 48 h). After each time, the cell survival was estimated by the colorimetric MTS assay, as previously reported [Chelli et al., 2004]. Each drug concentration was tested in duplicate and the experiments were repeated, at least, three times.

Transmission electron microscope analyses. After ADF cell exposure to 100 μM PK 11195 or to ethanol (1% v/v) (control) for increasing incubation times, both floating and adherent cells were collected by centrifugation. The pellets were washed in PBS and fixed as previously described [Chelli et al., 2005]. Ultrathin sections

were placed on Formvar carbon-coated nickel grids, stained with uranyl acetate and lead citrate and observed under a Jeol 100 SX transmission electron microscope (Jeol, Ltd, Japan).

Dot-blot experiments. Supernatants (0.5 ml) from control or 100 μM PK 11195 treated cells for 24 h were recovered and centrifuged to eliminate floating cells and cellular debris and then they were precipitated with acetone. Two microlitres of each supernatant were spotted onto a nitrocellulose membrane. After drying, the membranes were blocked for 3 h in 5% blotting-grade blocker non-fat dry milk and incubated overnight with a 1:3000 dilution of anti-HMGB1 antibody in 1% blotting-grade blocker non-fat dry milk. After several washings in Tris-buffered saline (10 mM Tris–HCl, pH 8 and 150 mM NaCl) containing 0.05% Tween-20, the membranes were incubated with an anti-rabbit horseradish peroxidase conjugated secondary antibody at a dilution of 1:100,000. Cross-reactivity was detected using the SuperSignal West Dura Extended Duration Substrate. Densitometry analyses were performed using the Scion Image 1.63 program. Three independent experiments done in triplicate for each experimental condition were carried out.

Evaluation of cytochrome c release from mitochondria. Cell cytosolic and mitochondrial fractions were isolated by use of a mitochondria/cytosol fractionation kit, according to the manufacturer's instructions. The protein content of each fraction was determined according to Bradford [1976] and the cytochrome *c* release has been evaluated as previously described [Chelli et al., 2005]. The monoclonal mouse anti-cytochrome *c* antibody was used at 1: 400 and the HSP-conjugated IgG anti-mouse secondary antibody was used at 1: 35,000. Reactive proteins were visualised with enhanced chemiluminescence SuperSignal West Pico Substrate and quantification of cytochrome *c* (12 kDa immunoreactive band) was performed by densitometric scanning of autoradiograms with an image analysis system (GS-670 Bio-Rad).

DNA fragmentation assay. In order to investigate the nature of cell death induced by PK 11195 in ADF cells, DNA fragmentation, a typical hallmark of apoptosis, was evaluated. After cell treatment with PK 11195 100 μM for 48 h, apoptosis was measured by using a photometric enzyme immunoassay for the in vitro quantitative determination of cytoplasmic histone-associated DNA fragments (mono- and oligonucleosomes). In parallel, a sample of cells was treated with the pro-apoptotic agent Lonidamine at 300 μM, used as positive control. Results were from two different experiments performed in duplicate.

Mitochondrial membrane potential analyses by flow cytometry. Changes in mitochondrial membrane potential ($\Delta\Psi_m$) were analysed by a flow cytometer (FACScalibur, Becton Dickinson) using the specific potentiometric fluorescent dye JC-1, essentially as previously described [Chelli et al., 2004]. Specifically, the flow cytometry analyses were performed following treatment of wt, Mock, Scramble or TSPO-2-transfected ADF cells with increasing concentrations of PK 11195 (25–100 μM) for different times (12–48 h). In some preliminary experiments, each ADF cell line was exposed for 30 min to increasing concentrations (1–50 μM) of the uncoupling agent CCCP, and then used as positive control in all subsequent assays, at the doses corresponding to the relative IC_{50} values.

Data analyses. Scatchard analyses of saturation binding data, displacement curves, graphic presentation and statistical analyses were performed using the nonlinear multipurpose curve-fitting Graph-Pad Prism computer program (Graph Pad Software, version 4.0; San Diego, CA). In detail, for saturation binding studies one-site binding curve fitting was used. IC_{50} values were derived by semilog plots of ligand displacement experiment data. The Cheng and Prusoff equation [1973] was used to calculate K_i values. Statistical analyses were performed by one-way ANOVA or two-way ANOVA (repeated measure) with Bonferroni post-test, as appropriately specified in the relative figure legends. *P*-value <0.05 was considered statistically significant. All data are presented as mean ± SEM, derived from, at least, three independent experiments, done in duplicate.

RESULTS

TSPO CHARACTERISATION IN wt ADF CELLS

[^{3}H]PK 11195 binding characterisation. The presence of TSPO in wt ADF cells was investigated by radioligand binding assays using the high affinity TSPO radioligand PK 11195 as described in several cellular system [Olson et al., 1988; Broaddus and Bennett, 1990; Zisterer et al., 1998; Hardwick et al., 1999; Giusti et al., 2004]. The specific [^{3}H]PK 11195 binding to ADF cell membranes was detected. The optimal membrane protein content of 20 μg was determined and used for all subsequent binding experiments. [^{3}H]PK 11195 equilibrium binding parameters (dissociation constant, K_d; maximum number of binding sites, B_{max}) were then determined by Scatchard analysis of saturation binding data, whereof a representative example is shown in Figure 1. Specific [^{3}H]PK 11195 binding was found to be saturable, whereas non-specific binding

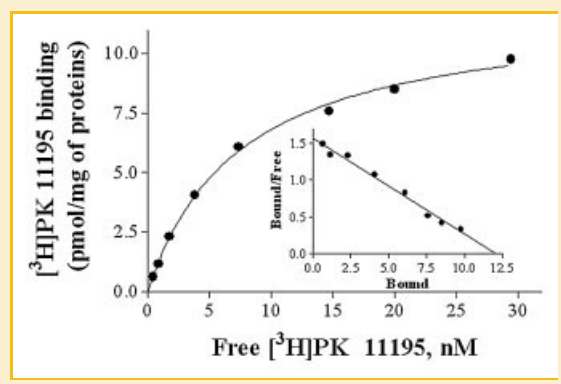

Fig. 1. Representative saturation curve and Scatchard plot (inset) of the specific [^{3}H]PK 11195 binding to wt ADF cell membranes. ($K_d = 7.71$ nM; $B_{max} = 12.1$ pmol/mg of proteins). ADF cell membranes (20 μg of proteins) were incubated with increasing concentrations of radioligand (ranging from 0.5 to 30 nM) for 90 min at 0°C. Non-specific binding was determined in the presence of 1 μM PK 11195. Three repeated experiments yielded similar results.

TABLE I. Pharmacological Characterisation of Specific [^{3}H]PK 11195 Binding to wt ADF Cell Membranes

Compounds	K_i (nM) mean ± SEM
PK 11195	3.59 ± 0.18
Ro5-4864	471.4 ± 46.9
Diazepam	2,000 ± 18.9
Clonazepam	>10,000

ADF cell membranes (20 μg of proteins) were incubated with [^{3}H]PK 11195 (1 nM) in the presence of different increasing drug concentrations. K_i (inhibition constant) were calculated from IC_{50} values by Cheng–Prusoff equation [1973]. Each value represents the mean ± SEM of three experiments done in duplicate.

increased linearly with the radioligand concentration and was less than 10% of total binding (data not shown). Scatchard analysis yielded a single straight-line plot indicating the presence of a homogenous population of binding sites. The mean K_d and B_{max} values were 7.58 ± 0.36 nM and 13.6 ± 1.03 pmol/mg of proteins, respectively. Furthermore, the existence of low-affinity [^{3}H]PK 11195 binding sites was also investigated using micromolar radioligand concentrations, essentially as previously described for other cell lines [Costa et al., 2006]. The obtained results did not evidence any specific low affinity binding sites in ADF cell membranes (data not shown).

Pharmacological characteristics of [^{3}H]PK 11195 binding sites in ADF cells were determined by competition experiments using different concentrations of classical TSPO ligands as displacers. The estimated K_i values for each competitive ligand are reported in Table I. In detail, PK 11195 showed a nanomolar rank order of potency with K_i of 3.59 ± 0.18 nM, whereas the benzodiazepine Ro5-4864 was less effective. [^{3}H]PK 11195 binding was displayed also by diazepam, but with low effectiveness, whereas Clonazepam, a selective central-type benzodiazepine receptor ligand, was not effective over the range of the concentrations studied.

Subcellular localisation of TSPO. Immunocytochemistry analysis revealed that in ADF cells the TSPO was distributed throughout the cytoplasm preferentially at the mitochondrial level (Fig. 2A). Indeed, the subcellular localisation of TSPO partially overlapped the pattern of mitochondria, as evidenced by anti-cytochrome *c* antibody staining (Fig. 2B,C).

TSPO FUNCTIONAL STUDIES IN wt ADF CELLS

Cell death induction by PK 11195. To assess the ability of the specific TSPO ligand PK 11195 to induce cell death, ADF cells were exposed to increasing ligand concentrations for different periods of time. Then, cell viability was quantitatively determined using MTS assay. Nanomolar PK 11195 concentrations (ranging from 1 to 100 nM) did not affect cell viability (data not shown), whereas micromolar ligand concentrations (from 1 to 100 μM) determined inhibition of cell survival. In particular, at short times (2, 6 or 12 h) PK 11195 affected cell viability with similar extent, causing, at the maximum tested ligand concentration, a reduction of cell viability of about 40% respect to controls (100%, untreated cells). Differently, PK 11195 caused an inhibition of ADF cell viability in a concentration- and time-dependent manner at prolonged time exposures. At the maximum tested ligand concentration and highest incubation time, the percentage of viable cells was reduced to 24.8 ± 4.42 versus control (Fig. 3). After each incubation time, the viability of untreated control cells resulted greater than 90% as verified by Trypan Blue exclusion assay (data not shown).

To evaluate the nature of cell death induced by PK 11195 in ADF cells, specific apoptotic markers were assayed. The mitochondrial potential dissipation ($\Delta\Psi_m$) was estimated by flow cytometry analysis using the specific mitochondrial potentiometric probe JC-1. A decrease in $\Delta\Psi_m$ is evidenced by a reduction in orange/red JC-1 aggregate fluorescence (recorded by FL-2 channel) and by a concomitant increase in green JC-1 monomer fluorescence (recorded by FL-1 channel), so that a decrease in red/green fluorescence ratio (FL-2/FL-1) value is measured. Following cell exposure to increasing micromolar PK 11195 concentrations (10–100 μM) for different periods of time (12, 24 or 48 h), a progressive dose- and time-dependent reduction in FL-2/FL-1 values was revealed, indicating that PK 11195 was able to induce mitochondrial potential dissipation in ADF cells (Fig. 4). Moreover, we quantified the release of cytochrome *c* from mitochondria in ADF cells exposed to PK 11195 by Western blot. As shown in Figure 5, ADF cell exposure to 100 μM PK 11195 for 24 h caused a release of cytochrome *c* from mitochondria, as revealed by comparing the density of the specific immunoreactive bands in the mitochondrial and cytosolic fractions. The amount of cytochrome *c* in cytosol of PK 11195 treated cells was 0.45 ± 0.067% as compared to 0.037 ± 0.0037% in untreated control cells ($P < 0.001$). In addition,

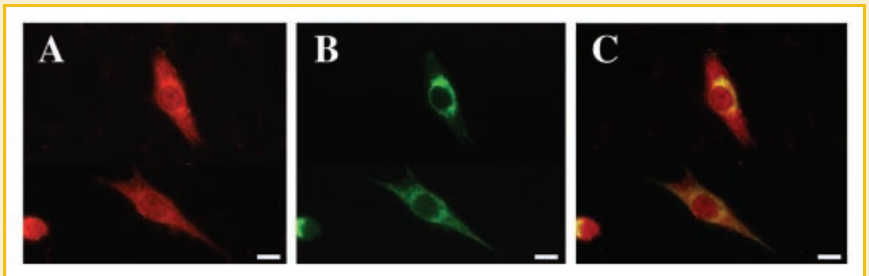

Fig. 2. Subcellular distribution analyses of TSPO in ADF cells by fluorescent microscopy. A: Distribution of TSPO as revealed by the use of anti-TSPO antibody. B: Subcellular distribution of mitochondria as revealed by the use of an anti-cytochrome *c* antibody. C: Merged panels A and B demonstrate that TSPO is preferentially localised in the mitochondria. Scale bars: 3.5 μm.

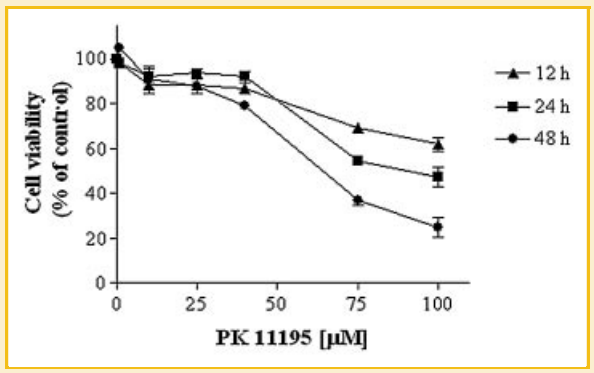

Fig. 3. Time course and dose–response of PK 11195-induced ADF cell death. Wt ADF cells were treated with increasing concentrations (1–100 μM) of PK 11195 for 12, 24 or 48 h. After each incubation time, cell viability was determined by MTS assay. The results are expressed as percentage of viable cells measured after PK 11195 treatment versus untreated control cells (100%) and shown as mean ± SEM, derived from, at least, three independent experiments done in duplicate.

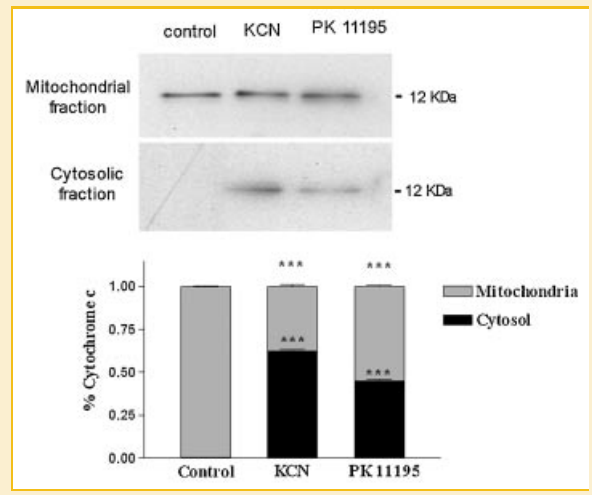

Fig. 5. Assessment of cytochrome *c* release from mitochondria by Western blot analysis. Wt ADF cells were exposed to either 100 μM PK 11195 (24 h) or 3.8 mM KCN (4 h). **A:** Cytochrome *c* was detected as a 12 kDa protein band by using a specific monoclonal antibody. **B:** For each individual sample, the immunoreactive band was densitometrically analysed, thus determining the percentage of cytochrome *c* in the cytosolic and mitochondrial fractions as a proportion of the total amount. $^{***}P < 0.001$ with respect to control cells, one-way ANOVA (Bonferroni post-test).

cytochrome *c* was also detected in the cytosol from cells exposed to 3.8 mM KCN for 4 h, used as positive control ($0.623 \pm 0.010\%$, $P < 0.001$). By prolonging exposure time of ADF cells to PK 11195, typical nuclear alterations of apoptosis were also detected. Indeed, ADF cell treatment with PK 11195 at 100 μM for 48 h resulted in a significant increase of DNA fragmentation respect to vehicle-treated control cells ($P < 0.01$; Fig. 6). As positive control, the cells were treated in parallel with 300 μM of the pro-apoptotic agent Lonidamine, which is a specific ligand of the PTP component adenine nucleotide translocator (ANT) [Del Bufalo et al.,1996]. The TEM analysis of ADF cells also confirmed the induction of apoptosis after prolonged PK 11195 cell exposure. Ultrastructural observations revealed that untreated ADF cells, as well as vehicle-treated cells (control), were irregularly round with large nuclei, abundant preserved endoplasmic reticulum and mitochondria with electrondense matrix and well preserved cristae (Fig. 7A). Following 24 h cell exposure to 100 μM PK 11195, ADF cells showed swollen endoplasmic reticulum and severely altered mitochondria still identifiable by the double membrane lacking the internal cristae

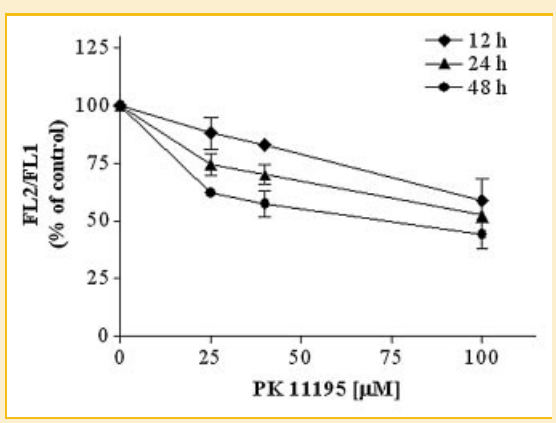

Fig. 4. Flow cytometry analyses of mitochondrial membrane potential dissipation by PK 11195 in wt ADF cells. After wt ADF cell exposure to increasing PK 11195 concentrations (25–100 μM) for different times, untreated (control) and treated cells were stained with JC-1. Both green (FL-1) and orange/red (FL-2) fluorescence emissions were simultaneously detected by a flow cytometer. $\Delta\Psi_m$ dissipation was expressed as FL-2/FL-1 value changes measured in PK 11195 treated ADF cells respect to controls, at which the arbitrary value of 100% was attributed. Data are shown as mean ± SEM, derived from, at least, three independent experiments done in duplicate.

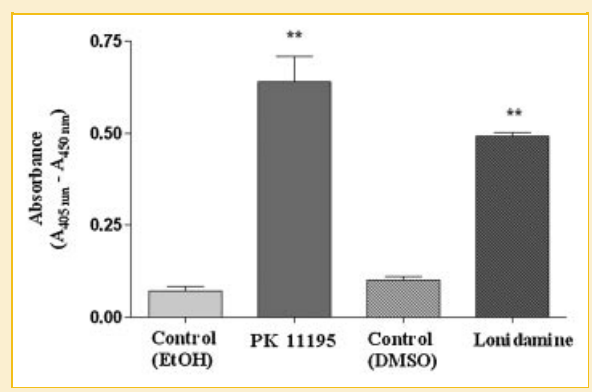

Fig. 6. Assessment of DNA fragmentation in ADF cells. Wt ADF cells were treated with PK 11195 100 μM, Lonidamine 300 μM or their respective vehicles (control) for 48 h. The used Lonidamine concentration corresponds to the dose able to inhibit the 50% (IC_{50} value) of ADF cell viability, as preliminarily determined. The determination of mono- and oligonucleosomes were determined using an ELISA kit as described in Materials and Methods Section. Data are shown as mean ± SEM, derived from at two independent experiment done in triplicate. $^{**}P < 0.01$ with respect to relative controls, one-way ANOVA (Bonferroni post-test).

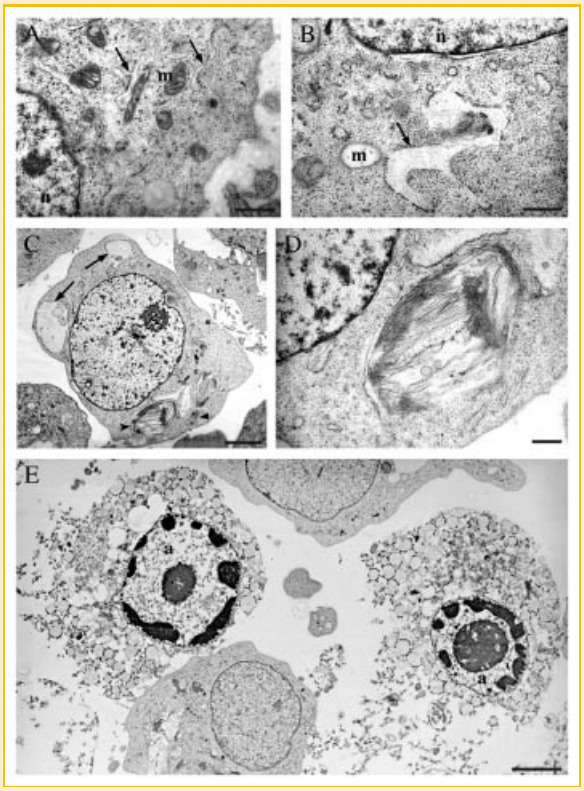

Fig. 7. Ultrastructural characteristics of PK 11195 treated ADF cells. Transmission electron microscopy (TEM) micrographs. A: Detail of an untreated ADF cell (control) showing some cisternae of rough endoplasmic reticulum (arrows) and mitochondria with well organised cristae and an electrondense matrix. B: Detail of an ADF cell exposed to 100 μM PK 11195 for 24 h showing a highly swollen endoplasmic reticulum (arrow) and altered mitochondria. C: An example of ADF cell treated with 100 μM PK 11195 for 48 h showing cytoplasmic degeneration with autophagic vacuoles (arrows) and multilamellar bodies at different stages of formation (arrowheads). D: Magnification of C. Detail of a multilamellar body containing thin electrondense lamellae. E: ADF cells after 72 h 100 μM PK 11195 exposure showing apoptotic nuclei (a), swollen cytoplasm and cell membrane rupture. Scale bars: 0.75 μm in A and D; 0.5 μm in B; 3 μm in C and E.

(Fig. 7B). Although cytoplasmatic alterations were visible, no evidence of chromatin condensation was observed at this time. After 48 h of PK 11195 treatment, autophagic vacuoles and multilamellar bodies, containing a large number of thin electrondense lamellae, were identified (Fig. 7C,D). Following PK 11195 treatment for 72 h, cells showed a typical apoptotic nucleus surrounded by a swollen cytoplasm. These cells showed evident plasma membrane breaks, a typical feature of necrosis, suggesting that a process of secondary necrosis occurred in vitro in the absence of phagocytosis (Fig. 7E).

In addition, to certainly exclude the necrosis, we analysed the eventual release of HMGB1 in the supernatants derived from ADF cells exposed to 100 μM PK 11195 for 24 h. Extracellular HMGB1 represents an optimal necrotic marker since it is passively released into the extracellular milieu by necrotic and damaged somatic cells. On the contrary, in cells undergoing apoptosis, chromatin irreversibly binds HMGB1, thereby ensuring that it will not diffuse away. Dot-blot analysis performed using an anti-HMGB1 antibody revealed that, following 24 h cell exposure to PK 11195 or to the known apoptotic agent vincristine (0.2 μM), no detectable signal was evident in the supernatants. On the contrary, a strong signal was detected in supernatants recovered from ADF cells treated with 0.8% Triton X-100 for 45 min, used as necrotic control cells (Fig. 8).

ADF CELL ENGINEERED TO REDUCE TSPO EXPRESSION

Transfection and TSPO expression level evaluation. Two siRNAs (TSPO-1 and TSPO-2) against distinct regions of TSPO sequence were developed and synthesised, and a Scramble siRNA with no homology to any mammalian sequence was used as negative control. The double-stranded siRNAs at concentrations of 10, 20, 50 or 100 nM were transfected into ADF cells for 72 h and intracellular flow cytometry analyses of protein expression were initially performed to select the most efficient siRNA. These assays revealed that both TSPO siRNAs reduced TSPO expression levels in a dose-dependent manner, and independent experiments showed that a 10 nM siRNA concentration was already efficient to reduce TSPO expression. However, the TSPO-2 siRNA resulted the most potent in TSPO silencing, therefore it was chosen for all the subsequent functional experiments. On the contrary, cell transfection with Scramble siRNA did not have any detectable effect on TSPO expression (data not shown).

Subsequently, to quantify the TSPO-2 siRNA efficacy to reduce TSPO expression levels and to test the silencing specificity, radioligand binding assays were performed. The specific [^{3}H]PK 11195 binding to ADF cell membranes, prepared from wt, Mock, Scramble and TSPO siRNAs treated cells, was measured at 72 and 120 h from transfection. As showed in Figure 9, 72 h after transfection the specific [^{3}H]PK 11195 binding was approximately

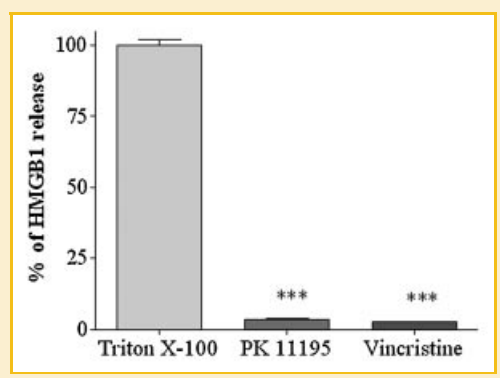

Fig. 8. Assessment of HMGB1 release in the supernatants derived from ADF cells exposed to 100 μM PK 11195 by dot-blot assays. The release was determined using an anti-HMGB1 antibody and the cross-reactivity was assessed by densitometry analysis. The results are expressed as percentage of the measured anti-HMGB1 cross-reactivity in the supernatants obtained from PK 11195- and vincristine-treated cells versus cells treated with 0.8% Triton X-100 at which the arbitrary value of 100% was attributed. Data are shown as mean ± SEM, derived from at least three independent experiment done in duplicate. $^{***}P < 0.001$ with respect to Triton X-100-treated cells, one-way ANOVA (Bonferroni post-test).

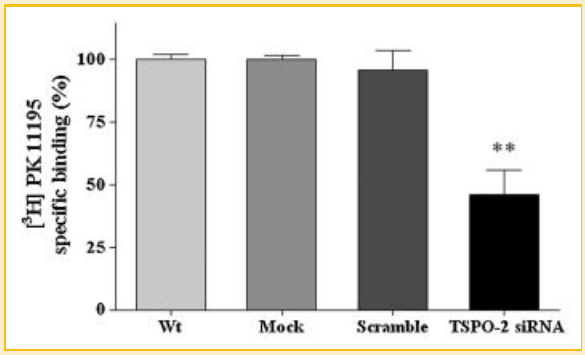

Fig. 9. Assessment of TSPO silencing in ADF cells by radioligand binding assays. The specific [^{3}H]PK 11195 binding to wt, Mock, Scramble and TSPO-2 siRNA ADF cell membranes was determined. The results are expressed as percentage of the specific [^{3}H]PK 11195 binding measured in Mock, Scramble and TSPO-2 siRNA versus wt cells at which the arbitrary value of 100% was attributed. Data are obtained from at least three independent experiments, done in duplicate. Each bar represents the mean value ± SEM. $^{**}P < 0.01$ with respect to control cells, one-way ANOVA (Bonferroni post-test).

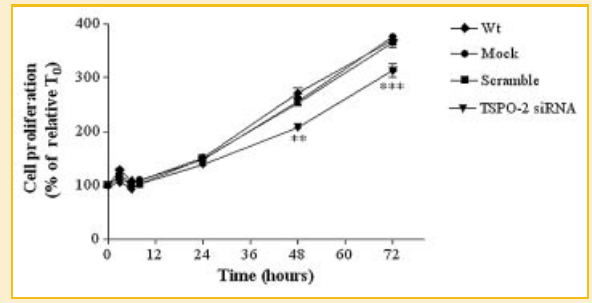

Fig. 10. Cell proliferation rate in TSPO silenced and control cells. The same amounts of wt, Mock, Scramble and TSPO-2 siRNA ADF cells were seeded and allowed to proliferate for 72 h. After cell incubation with the MTS reagent, the proliferation of each ADF cell line was determined at different times measuring the absorbance at 490 nm. For each cell line, the results were normalised to the respective absorbance value measured at the starting time of assay (T_0), at which the value of 100% was attributed. Data are shown as mean ± SEM, derived from, at least, three independent experiments done in duplicate. $^{**}P < 0.01$, $^{***}P < 0.001$ with respect to control cells, two-way ANOVA (repeated measure) (Bonferroni post-test).

reduced of 54% in cells transfected with TSPO-2 siRNA ($P < 0.01$ vs. control cells). On the contrary, no significant effect was observed in Scramble cells ($P > 0.05$ vs. Mock or wt cells). Therefore, a twofold reduction of [^{3}H]PK 11195 binding in TSPO-2 siRNA-treated cells was evidenced respect to control cells. The [^{3}H]PK 11195 binding in TSPO silenced cells was still reduced 120 h after transfection indicating that the silencing efficiency was retained at this time (data not shown).

FUNCTIONAL STUDIES IN TSPO SILENCED AND CONTROL ADF CELL LINES

Cell proliferation. With the aim to analyse the relationship between TSPO expression levels and cell growth, we assessed the proliferation rate of TSPO-2 siRNA transfected cells as well as of wt, Mock and Scramble ADF cells by using the MTS assay. As reported in Figure 10, differences in the proliferation rate were evidenced among TSPO-2 siRNA transfected ADF cells and control cells. In particular, wt, Mock and Scramble cells grew similarly and proliferated faster than the TSPO silenced ADF cells. Significant differences appeared 48 h after seeding (time zero, T_0; $P < 0.01$). Cell viability analysis, performed by Trypan Blue test, showed that the percentage of dead cells was about 5% in each ADF cell line at the time of cell seeding, and that the number of dead cells was similar among wt, mock, Scramble and TSPO silenced cells at each time analysed.

Cell death induction by PK 11195. To assess the specific PK 11195 efficacy to induce death in ADF cells, we evaluated its effect on cell viability in TSPO silenced cells in comparison with Scramble, Mock and wt cells by MTS assays. Interestingly, we observed that the susceptibility of TSPO-2 siRNA transfected cells to the anti-proliferative activity of PK 11195 was significantly reduced in comparison to those shown by wt, Scramble or Mock cells. This difference was observed at each time of PK 11195 cell exposure, however, it resulted greater in magnitude at short time of treatment. In detail, in Figure 11 are reported the data obtained after 12 h cell treatment showing that at low doses (10 and 25 μM) PK 11195 was completely ineffective on TSPO silenced ADF cells. On the contrary, increased PK 11195 doses were able to induce cell viability inhibition in TSPO silenced ADF cells too, although this effect was less marked with respect to control cells.

Mitochondrial membrane susceptibility to depolarisation in TSPO-silenced cells. Since mitochondrial membrane potential plays a key role in the control of apoptotic response, we evaluated

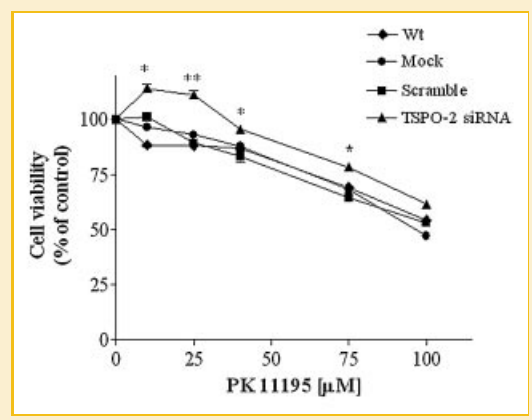

Fig. 11. Cell viability inhibition by PK 11195 in TSPO silenced and control cells. Wt, Mock, Scramble and TSPO-2 siRNA ADF cells were treated with increasing PK 11195 concentrations (10–100 μM) for 12 h and then the cell viability was determined by MTS assay. For each cell line, the results are expressed as percentage of viable cells measured after PK 11195 treatment versus respective untreated control cells (100%) and shown as mean ± SEM, derived from at least three independent experiment, done in duplicate. $^{*}P < 0.05$; $^{**}P < 0.01$ with respect to control cells, two-way ANOVA (repeated measure) (Bonferroni post-test).

the susceptibility to potential dissipation of TSPO-silenced cells in comparison to control cells (wt, Mock and Scramble cells) with the aim to better elucidate the role of TSPO in apoptosis induction in ADF cells.

By using the mitochondrial potentiometric probe JC-1, as described above, we found a different PK 11195 efficacy to induce mitochondrial potential dissipation depending on TSPO levels. As reported in Figure 12, PK 11195 treatment (12 h) was less effective to induce $\Delta\Psi_m$ in TSPO-silenced ADF cells in comparison with control cells. The different TSPO-siRNA mitochondrial sensitivity was evidenced in response to the well-known uncoupling agent CCCP, too. In fact, CCCP concentrations required to reduce the untreated cell fluorescence value to 50% (IC_{50}) were different between TSPO silenced and control cells, with mean values of 3.46 ± 1.21 μM for wt, 4.42 ± 1.18 μM for Mock, 5.56 ± 1.38 μM for Scramble and 13.4 ± 1.01 μM for TSPO-2-transfected ADF cells.

DISCUSSION

Tumours of glial origin are characterised by a rapid invasive growth into the surrounding brain parenchyma and by a frequent resistance to the standard therapies. Technological advances in oncogenomics, proteomics and functional genomic screens are providing mechanisms to rapidly identify the critical targets whose inactivation will lead to a substantive glioma growth arrest. However, the understanding of the complex molecular pathways involved in this tumour transformation and progression is still an open question. In this field new findings will be fundamental to give new clues to develop targeted therapies against this still untreatable cancer. In this line, we focalised our attention on TSPO as in the brain it is exclusively expressed in glial cells and is over-expressed in gliomas [Brown et al., 2000; Veenman et al., 2004; Veenman and Gavish, 2006; Vlodavsky and Soustiel, 2007]. Therefore, TSPO may

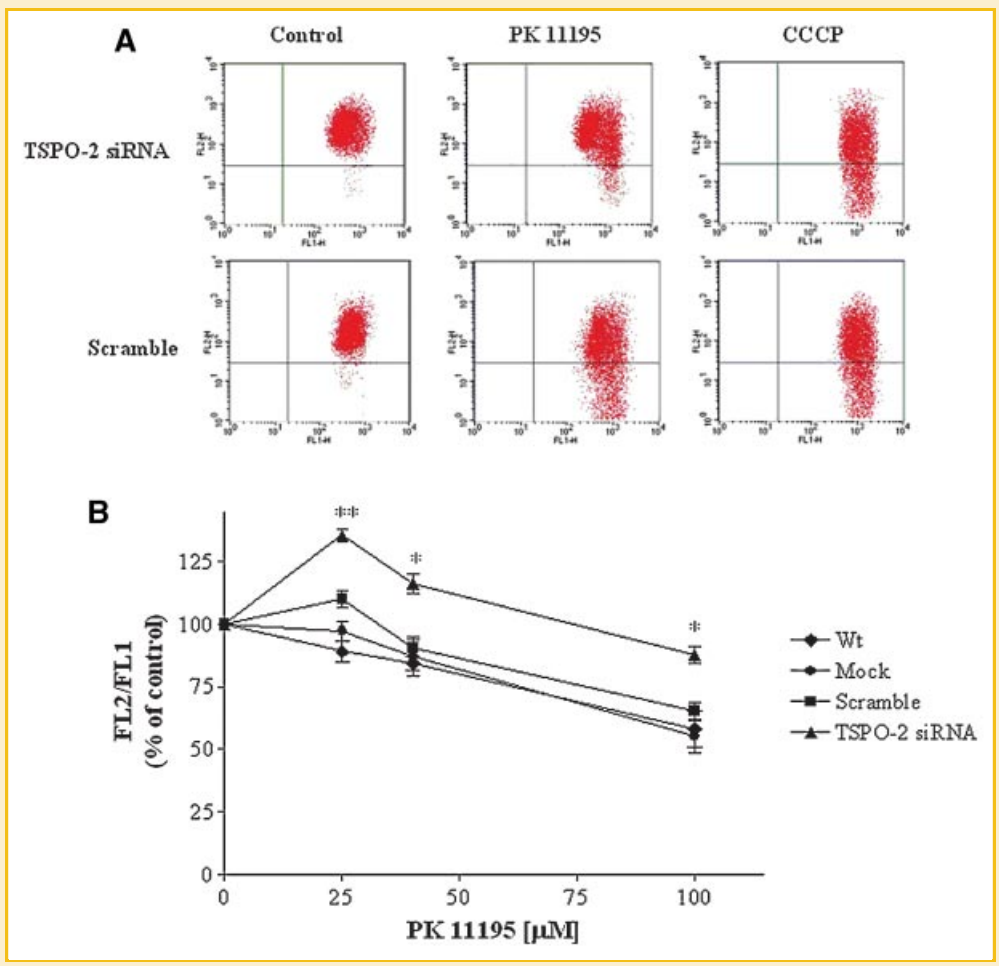

Fig. 12. Flow cytometry analyses of mitochondrial membrane potential dissipation by PK 11195 in TSPO-silenced and control cells. Following wt, Mock, Scramble and TSPO-2 ADF cell treatment with increasing PK 11195 concentrations (25–100 μM) for 12 h, the cells were stained with JC-1. A: Representative examples of dot-blots of the fluorescence pattern of TSPO-siRNA and Scramble cell untreated (control) or treated with PK 11195 (100 μM) or CCCP (at the concentrations corresponding to the relative IC_{50} values). Cells with polarised mitochondria are found in the upper right quadrant of plots, corresponding to high fluorescence emission both in FL-1 (green; *x*-axis) and FL-2 (orange; *y*-axis) channels. After PK 11195 treatment, mitochondrial depolarisation is visible by a decrease in the fluorescence emission in the FL-2 channel and an increase in the FL-1 channel. B: Dose–response curves of $\Delta\Psi_m$ dissipation by PK 11195 measured in each ADF cell line. $\Delta\Psi_m$ dissipation, expressed as FL-2/FL-1 values, was determined as described in the legend of Figure 4. Data are shown as mean ± SEM, derived from, at least, three independent experiments done in duplicate. $^{*}P < 0.05$, $^{**}P < 0.01$ with respect to control cells, two-way ANOVA (repeated measure) (Bonferroni post-test). [Color figure can be viewed in the online issue, which is available at www.interscience.wiley.com.]

represent a promising protein target to develop a specific-cell anti-cancer strategy. Here, we firstly characterised pharmacological features of TSPO in a human astrocytoma cell line, the ADF cells. [^{3}H]PK 11195 bound to cell membranes in a protein dependent and saturable manner with the same pharmacological profile specificity reported in other human glioma cells [Olson et al., 1988; Broaddus and Bennett, 1990; Zisterer et al., 1998] as well as in other human tumoural or normal cell types [Broaddus and Bennett, 1990; Hardwick et al., 1999; Giusti et al., 2004]. [^{3}H]PK 11195 saturation isotherms revealed a single class of binding sites with high affinity and density. PK 11195 low-affinity binding sites, which have been previously described in leukaemia cell line by our group [Costa et al., 2006], was not evidenced even at high radiolabelled ligand concentrations.

TSPO was preferentially expressed in ADF cells at mitochondrial level, which has been reported to be the primary subcellular localisation of this protein [Casellas et al., 2002; Veenman and Gavish, 2006]. Indeed, TSPO constitutes a main component of the mitochondrial PTP, whose opening induces loss of mitochondrial potential and triggers the cascade of biochemical events leading to apoptotic cell death [Galluzzi et al., 2006]. In line with these evidences, we demonstrated that PK 11195 inhibited cell survival, caused dissipation of mitochondrial membrane potential in a dose- and time-dependent manner and the release of cytochrome *c* from mitochondria, suggesting an action of PK 11195 via PTP modulation. Mitochondrial alterations were also revealed by ultrastructural analyses, which showed the presence of swollen and disorganised mitochondria. These ultrastructural alterations paralleled with the presence in the cytoplasm of autophagic vacuoles suggesting an activation of an autophagic/apoptotic pathway during which the accumulation of autophagic vacuoles might precede apoptotic cell death. Typical nuclear features of apoptosis were evident after a prolonged PK 11195 treatment as demonstrated by the nuclear DNA fragmentation and the absence of the specific necrotic marker HMGB1 expression in the extracellular milieu of PK 11195-treated ADF cells.

All these data indicate that micromolar TSPO ligand PK 11195 concentrations affect human ADF cell survival triggering apoptotic pathway as also previously evidenced in rat C6 glioma cells [Chelli et al., 2004]. On the contrary, nanomolar PK 11195 concentrations were unable to inhibit cell survival. The observed discrepancy between the micromolar PK 11195 concentrations able to induce cell death and the nanomolar binding affinity shown by TSPO ligands has been also previously described and debated. In fact, despite the nanomolar affinity of PK 11195 and of other TSPO ligands, it is commonly known that they show anti-proliferative and pro-apoptotic activity, as well as steroidogenic action, at saturating (micromolar) doses higher than those expected from their affinity to the protein [Landau et al., 1998; Maaser et al., 2001; Sutter et al., 2002; Primofiore et al., 2004; Veenman et al., 2007]. However, the actual meaning of this discrepancy is still understood.

Since TSPO expression levels have been positively correlated with glioma progression and aggressiveness [Brown et al., 2000; Veenman et al., 2004], the role of TSPO expression levels on ADF cell growth and susceptibility to undergo cell death were explored. For these purposes, ADF cells were engineered to express reduced TSPO levels through siRNA technique. The success in TSPO silencing was demonstrated by the significant reduction of [^{3}H]PK 11195 specific binding, which reveals a reduced protein amount. The TSPO silencing was stable for several days following trasfection, allowing us to perform functional assays on these cell lines. In detail, proliferation assays indicated that TSPO-2 siRNA transfected cells showed a decreased proliferation rate without changes in the number of dead cells. This finding demonstrates that TSPO expression levels positively correlates with the cell proliferation rate as previously hypothesised by indirectly comparing various tumoural cells expressing different TSPO densities with their different malignancy grades [Hardwick et al., 1999; Veenman et al., 2004]. Furthermore, TSPO silencing caused a different ADF cell susceptibility to cell death as revealed by PK 11195 reduced ability in inhibiting cell survival. An hypothesis is that the reduced TSPO expression level determines a change of PTP structural conformation that alters the threshold of PTP transition and, so the cell resistance to mitochondrial potential dissipation and the subsequent apoptosis induction. In line with this hypothesis, we evidenced that a reduction of TSPO expression resulted in an higher cell resistance to mitochondrial depolarisation induced by PK 11195 or by the known uncoupling agent CCCP, indicating that mitochondria of TSPO-silenced cell depolarise less readily. In accordance with this issue, our unpublished data revealed that ADF TSPO-silenced cells were also less sensitive to the anti-proliferative effect induced by Lonidamine, which is a specific ligand of the ANT protein associated with TSPO in PTP structure. The relation between cell susceptibility to TSPO ligand and protein density revealed in our study agree with previously data. Veenman et al. [2004] reported that the specific TSPO ligand Ro5-4864 differentially reduced basal apoptosis in different glioma cell lines expressing various TSPO densities and Fischer et al. [2001] demonstrate that the PK 11195 pro-apoptotic potency paralleled with the level of transient TSPO expression during hepatic stellate cell transformation. In addition, according to our results, recent reports demonstrate that TSPO down-regulation influences cell survival and proliferation of human breast cancer cells [Li et al., 2007] and diminishes the extent of mitochondrial potential loss and cell swelling in cultured astrocytes following ammonia treatment [Panickar et al., 2007]. Interestingly, 25 μM PK 11195 concentration appeared to affect differentially mitochondrial potential in TSPO silenced ADF cells. At this dose PK 11195 seemed to induce mitochondrial polarisation instead of depolarisation, suggesting that low doses of TSPO ligands can elicit a protective activity. Indeed, contrasting effects of some TSPO ligands, including PK 11195, on apoptosis have been recently reported in many different tumoural cell types [Veenman and Gavish, 2006].

In conclusion, our findings demonstrate that PK 11195 induces cell death via autophagic/apoptosis pathway in a human astrocytoma cell line by modulating PTP opening and that different TSPO expression levels influence the tumoural cell proliferation rate and the susceptibility to death induction. The efficacy of PK 11195 to differentially affect cell viability in relation to different TSPO expression levels appears to be particularly important being PK 11195 frequently proposed, by several authors, as a promising chemotherapy agent.

ACKNOWLEDGMENTS

We are especially grateful to Dr M.C. Iorio and M. Evangelista for their help in performing flow cytometry analyses; C. Ghezzani for his technical assistance in the electron microscopy techniques, A. Mercatanti for siRNA sequence identification and Dr Cristofani for statistical data analyses.

REFERENCES

Bradford MM. 1976. A rapid and sensitive method for the quantitation of microgram quantities of protein utilizing the principle of protein-dye binding. Anal Biochem 72:248–254.

Broaddus WC, Bennett JP, Jr. 1990. Peripheral-type benzodiazepine receptors in human glioblastomas: Pharmacologic characterization and photoaffinity labeling of ligand recognition site. Brain Res 518:199–208.

Brown RC, Degenhardt B, Kotoula M, Papadopoulous V. 2000. Location-dependent role of the human glioma cell peripheral-type benzodiazepine receptor in proliferation and steroid biosynthesis. Cancer Lett 156:125–132.

Casellas P, Galiegue S, Basile AS. 2002. Peripheral benzodiazepine receptors and mitochondrial function. Neurochem Int 40:475–486.

Ceruti S, Franceschi C, Barbieri D, Malorni W, Camurri A, Giammarioli AM, Ambrosini A, Racagni G, Cattabeni F, Abbracchio MP. 2000. Apoptosis induced by 2-chloro-adenosine and 2-chloro-2′-deoxy-adenosine in a human astrocytoma cell line: Differential mechanisms and possible clinical relevance. J Neurosi Res 60:388–400.

Chelli B, Lena A, Vanacore R, Da Pozzo E, Costa B, Rossi L, Salvetti A, Scatena F, Ceruti S, Abbracchio MP, Gremigni V, Martini C. 2004. Peripheral benzodiazepine receptor ligands: Mitochondrial transmembrane potential depolarization and apoptosis induction in rat C6 glioma cells. Biochem Pharmacol 68:125–134.

Chelli B, Rossi L, Da Pozzo E, Costa B, Spinetti F, Rechichi M, Salvetti A, Lena A, Simorini F, Vanacore R, Scatena F, Da Settimo F, Gremigni V, Martini C. 2005. PIGA (N,N-di-n-butyl-5-chloro-2-(4-chlorophenyl)indol-3-ylglyoxylamide), a new mithocondrial Benzodiazepine receptor ligand, induces apoptosis in C6 glioma cells. ChemBiochem 6:1–8.

Cheng YC, Prusoff WH. 1973. Relationship between the inhibition constant (Ki) and the concentration of the inhibitor which causes 50% inhibition (IC_{50}) of an enzymatic reaction. Biochem Pharmacol 22:3099–3108.

Costa B, Salvetti A, Rossi L, Spinetti F, Lena A, Chelli B, Rechichi M, Da Pozzo E, Gremigni V, Martini C. 2006. Peripheral benzodiazepine receptor: Characterization in human T-lymphoma Jurkat Cells. Mol Pharmacol 69: 37–44.

Decaudin D. 2004. Peripheral benzodiazepine receptor and its clinical targeting. Anticancer Drugs 15:737–745.

Del Bufalo D, Biroccio A, Soddu S, Laudonio N, D'Angelo C, Sacchi A, Zupi G. 1996. Lonidamine induces apoptosis in drug-resistant cells independently of the p53 gene. J Clin Invest 98(5):1165–1173.

Elbashir SM, Harborth J, Weber K, Tuschl T. 2002. Analysis of gene function in somatic mammalian cell using small interfering RNA. Methods 26:199–213.

Fischer R, Schmitt M, Bode JG, Haussinger D. 2001. Expression of the peripheral-type benzodiazepine receptor and apoptosis induction in hepatic stellate cells. Gastroenterology 120:1285–1288.

Galiegue S, Tinel N, Casellas P. 2003. The peripheral benzodiazepine receptor: A promising therapeutic drug target. Curr Med Chem 10:1563–1572.

Galluzzi L, Larochette N, Zamzami N, Kroemer G. 2006. Mitochondria as therapeutic targets for cancer chemotherapy. Oncogene 25:4812–4830.

Giusti L, Costa B, Viacava P, Castagna M, Iacconi P, Ricci RE, Zaccagnini M, Miccoli P, Lucacchini A. 2004. Peripheral type benzodiazepine receptor in human parathyroid glands: Up-regulation in adenoma. J Endocrinol Invest 27:826–831.

Hardwick M, Fertikh D, Culty M, Li H, Vidic B, Papadopoulos V. 1999. Peripheral-type benzodiazepine receptor (PBR) in human breast cancer: Correlation of breast cancer cell aggressive phenotype with PBR expression, nuclear localization, and PBR-mediated cell proliferation and nuclear transport of cholesterol. Cancer Res 59:831–842.

Landau M, Weizman A, Zoref-Shani E, Beery E, Wasseman L, Landau O, Gavish M, Brenner S, Nordenberg J. 1998. Antiproliferative and differentiating effects of benzodiazepine receptor ligands on B16 melanoma cells. Biochem Pharmacol 56:1029–1034.

Li W, Hardwick MJ, Rosenthal D, Culty M, Papadopoulos V. 2007. Peripheral-type benzodiazepine receptor overexpression and knockdown in human breast cancer cells indicate its prominent role in tumor cell proliferation. Biochem Pharmacol 73:491–503.

Maaser K, Höpfner M, Jansen A, Weisinger G, Gavish M, Kozikowski AP, Weizman A, Carayon P, Riecken EO, Zeitz M, Scherübl H. 2001. Specific ligands of the peripheral benzodiazepine receptor induce apoptosis and cell cycle arrest in human colorectal cancer cells. Br J Cancer 85:1771–1780.

Malorni W, Rainaldi G, Rivabene R, Santini MT. 1994. Different susceptibilities to cell death induced by t-butylhydroperoxide could depend upon cell histotype-associated growth features. Cell Biol Toxicol 10:207–218.

Olson JM, Junck L, Young AB, Penney JB, Mancini WR. 1988. Isoquinoline and peripheral-type benzodiazepine binding in gliomas: Implications for diagnostic imaging. Cancer Res 48:5837–5841.

Panickar KS, Jayakumar AR, Rama Rao KV, Norenberg MD. 2007. Down-regulation of the 18-kDa translocator protein: Effects on the ammonia-induced mitochondrial permeability transition and cell swelling in cultured astrocytes. Glia 55:1720–1727.

Papadopoulos V, Baraldi M, Guilarte TR. 2006a. Translocator protein (18kDa): New nomenclature for the peripheral-type benzodiazepine receptor based on its structure and molecular function. Trends Pharmacol Sci 27:402–409.

Papadopoulos V, Lecanu L, Brown RC, Han Z, Yao ZX. 2006b. Peripheral-type benzodiazepine receptor in neurosteroid biosynthesis, neuropathology and neurological disorders. Neuroscience 138:749–756.

Poliseno L, Evangelista M, Mercatanti A, Mariani L, Citti L, Rainaldi G. 2004. The energy profiling of short interfering RNA is highly predictive of their activity. Oligonucleotides 14:227–232.

Poliseno L, Evangelista M, Ricci F, Bonotti A, Nannipieri M, Rainaldi G. 2005. Identification of active siRNAs against IGF-IR of porcine coronary smooth muscle cells in a heterologous cell line. Int J Mol Med 15:713–738.

Primofiore G, Da Settimo F, Taliani S, Simorini F, Patrizi MP, Novellino E, Greco G, Abignente E, Costa B, Chelli B, Martini C. 2004. N,N-dialkyl-2-phenylindol-3-ylglyoxylamides. A new class of potent and selective ligands at the peripheral benzodiazepine receptor. J Med Chem 47:1852–1855.

Stern JI, Raizer JJ. 2006. Chemotherapy in the treatment of malignant gliomas. Expert Rev Anticancer Ther 6:755–767.

Sutter AP, Maaser K, Höpfner M, Barthel B, Grabowski P, Faiss S, Carayon P, Zeitz M, Scherübl H. 2002. Specific ligands of the peripheral benzodiazepine receptor induce apoptosis and cell cycle arrest in human esophageal cancer cells. Int J Cancer 102:318–327.

Veenman L, Gavish M. 2006. The peripheral-type benzodiazepine receptor and the cardiovascular system. Implications for drug development. Pharmacol Ther 110:503–524.

Veenman L, Levin E, Weisinger G, Leschiner S, Spanier I, Snyder SH, Weizman A, Gavish M. 2004. Peripheral-type benzodiazepine receptor density and in vitro tumorigenicity of glioma cell lines. Biochem Pharmacol 68:689–698.

Veenman L, Papadopoulos V, Gavish M. 2007. Channel-like functions of the 18-kDa translocator protein (TSPO): Regulation of apoptosis and steroidogenesis as part of the host-defense response. Curr Pharm 13:2385–2405.

Vlodavsky E, Soustiel JF. 2007. Immunohistochemical expression of peripheral benzodiazepine receptors in human astrocytomas and its correlation with grade of malignancy, proliferation, apoptosis and survival. J Neurooncol 81:1–7.

Zisterer DM, Hance N, Campiani G, Garofalo A, Nacci V, Williams DC. 1998. Antiproliferative action of pyrrolobenzoxazepine derivatives in cultured cells: Absence of correlation with binding to the peripheral-type benzodiazepine binding site. Biochem Pharmacol 55:397–403.

Zoratti M, Szabo I. 1995. The mitochondrial permeability transition. Biochim Biophys Acta 1241:139–176.